CrI_3 Magnetic Nanotubes: A Comparative DFT and DFT+U study, and strain effect

Artem V. Kuklin[a,b,*], Maxim A. Visotin[a,c], Woohyeon Baek[d], Paul V. Avramov[d]

[a]*Division of Theoretical Physics and Wave Phenomena, Siberian Federal University, 79 Svobodniy av., Krasnoyarsk 660041, Russia*

[b]*Division of Theoretical Chemistry and Biology, School of Engineering Sciences in Chemistry, Biotechnology and Health, KTH Royal Institute of Technology, 10691 Stockholm, Sweden*

[c]*Federal Research Center KSC Siberian Branch Russian Academy of Sciences, 660036 Krasnoyarsk, Russia*

[d]*Department of Chemistry and Green-Nano Materials Research Center, Kyungpook National University, 80 Daehak-ro, Buk-gu, Daegu, 41566, South Korea*

**e-mail*: artem.icm@gmail.com

Abstract

In this paper, structural and electronic properties of CrI_3 magnetic nanotubes (NTs) are studied using density functional theory. Both armchair and zigzag CrI_3 nanotubes demonstrate a high correlation in strain energy between each other independently on accounting the Hubbard correction. The strain energies decrease with expansion of the tube diameter making the tubes' synthesis with a diameter larger than 45 Å to be energetically possible. The nanotubes of both zigzag and armchair chirality are ferromagnetic semiconductors with band gaps close to that of the CrI_3 monolayer. The band gaps are suppressed by reducing the tube diameters due to the structural stress leading to deformation of the Cr-I crystal field and changes in the bond lengths. The external strain can be utilized to flexibly tune the electronic properties of CrI_3 nanotubes with desired spin-up/spin-down band gap ratio. Strong distortion of the octahedral Cr-I crystal field under compression results in nontrivial behavior in the spin-up band gap of (4, 4) tube. Moreover stretching of tubes leads to the enhancement of the exchange energy that should result in higher Curie temperature, therefore providing a good platform for potential application in spintronic nanodevices.

I. INTRODUCTION

Discovery of carbon nanotubes (CNTs) [1] and their following intensive investigations led to a new field in condensed matter physics represented by one-dimensional objects. Nanotubes can be open or closed, contain five-membered rings, they can be single- or multi-walled [2,3]. Later, nanotubes based on other inorganic materials including BN nanotubes [4–6] and nanotubes based on transition metal dichalcogenides (TMD) were found as well. The latter ones contain a layer of metal ions between two layers of chalcogen in the trigonal pyramidal or octahedral coordination position. Tubular-like structures of MoS_2 reported by Chianelli [7]. who studied their application in catalysis. However, the first inorganic nanotubes successfully obtained from complex layered compounds such as WS_2 and MoS_2 reported by Tenne [8,9]. Such nanotubes have been well theoretically described by G. Seifert et al. [10,11]. Single wall TMD nanotubes have remarkable electronic properties depending on their diameter and chirality. While nanotubes with chirality "zigzag" (n, 0) are direct bandgap semiconductors, "armchair" (n, n) ones are closer to two-dimensional (2D) TMD [12]. The band gap increases with an increase in diameter of the tubes, and it approaches that in the monolayer for diameters greater than 40 Å.

The recent synthesis of the first ferromagnetic two-dimensional materials such as $Cr_2Ge_2Te_6$ and CrI_3 [13,14] opens a new chapter in the physics of low-dimensional materials. Among them, CrI_3 is the most interesting in terms of dimension-related and magnetic properties due to antiferromagnet-ferromagnet transition in the monolayer [15]. In addition, several low-dimensional magnets were recently predicted theoretically [16–19] and realized experimentally [20–22] along with complex heterostructures [23–26]. The integration of magnetic ordering into two-dimensional heterostructures [27] exhibits vast possibilities for development of new devices based on new physical phenomena. Crystalline CrI_3 is a layered material with ferromagnetic ordering and T_C=61 K [28]. It has been shown that the ferromagnetic order is preserved in mechanically cleaved CrI_3 monolayers, while the Curie temperature decreases to T_C=45 K [14]. Experimental results and DFT calculations demonstrate that CrI_3 is a semiconductor material with a band gap of 1.2 eV [14,29]. Similar to transition metal dichalcogenides the CrI_3 monolayer could be folded into a nanotube preserving of its magnetic order and generating new one-dimensional ferromagnetic materials for valuable nanoelectronic applications.

In this paper, the structural, energy and electronic properties of CrI_3 magnetic nanotubes are studied using the density functional theory. Folding the CrI_3 sheet into a tube leads to decrease of

the inner Cr-I bond lengths, whereas increasing outer ones and results in distortion of Cr-I crystal field. The strain energies of CrI_3 nanotubes of both chiralities are in a high correlation with their diameters independently on the Hubbard correction. Both types of nanotubes are ferromagnetic semiconductors with the band gap width close to that of the monolayer. Applying strain to the tubes one can flexibly vary the band gaps and exchange energies.

II. COMPUTATIONAL METODS

The electronic structure calculations were performed using density functional theory (DFT) [30,31] within GGA PBE [32,33] exchange functional and Hubbard correction (GGA + U) [34,35] in the form realized in Vienna Ab-initio Simulation Package (VASP) [36,37]. The parameters U=2.9 eV and J=0.7 eV were chosen based on recent RPA calculations [38], that provide quite accurate correlation contribution. The correction of van der Waals interaction by the Grimm D3 [39] method was used in simulations of the nanostructures. The plane-wave cutoff energy was set to 500 eV. To avoid interaction between the neighbor images of the nanotubes, the vacuum gap is specified >10 Å. The first Brillion zone is sampled to 1×1×4 and 1×1×40 *k*-points for geometry relaxations and electronic structure calculations, respectively, using the Monkhorst-Pack scheme [40]. The convergence criteria for forces acting on the atoms and electronic iterations were 10^{-2} eV/Å and 10^{-5} eV, respectively.

III. RESULTS AND DISCUSSION

In order to assess the accuracy of the chosen method, the layered structure of the bulk CrI_3 unit cell is optimized using the PBE+D3 functional. The equilibrium geometry of CrI_3 indicates that the resulting cell vectors (a = 6.886, b = 11.920 and c = 6.677 Å) are in good agreement with the experimental ones (a = 6.893, b = 11.927 and c = 6.984 Å) [28]. A relatively smaller distance along the c vector is probably due to the overestimation of the interlayer interaction energy. Applying the correlation parameter (PBE+U+D3), the cell vectors are a = 6.958, b = 12.024, and c = 6.723 Å. The obtained parameters indicate a slight overestimation of covalent bonding in CrI_3, while the van der Waals interactions are still underestimated. Based on the calculated equilibrium geometry of the CrI_3 unit cell, a two-dimensional cell, which can be represented as a hexagonal monolayer with the vector a = 6.904 Å and two Cr atoms in the unit cell, is designed and relaxed (Fig. 1a). A vacuum interval of ~20 Å is used to prevent any interactions between neighboring images.

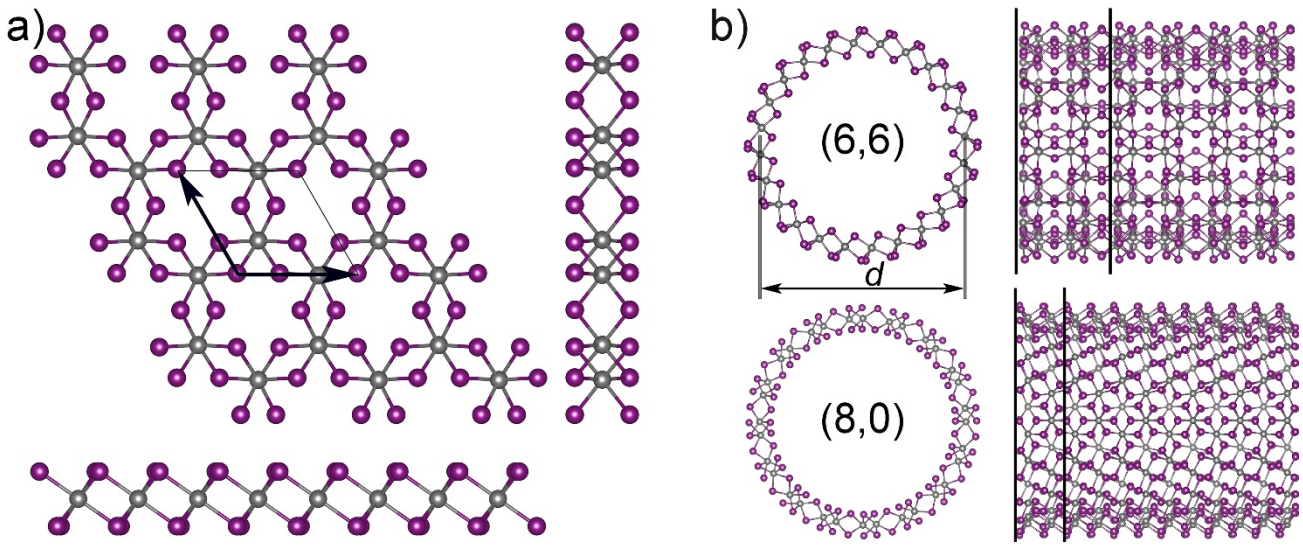

FIG. 1. The equilibrium geometries of (a) single-layer CrI_3 (top and side views). The black arrows represent translation vectors *a* and *b*. (b) (6, 6) armchair (top) and (8, 0) zigzag (bottom) CrI_3 nanotubes. The blue and gray atoms represent I and Cr respectively. The unit cells are marked with solid black lines.

Similar to other materials like graphene and TMDs, CrI_3 nanotubes (Fig. 1b) can be designed by folding a monolayer along a certain direction described by two indices $B=na+ma$. Following the notation of nanotube chirality, (n, n) and (n, 0) correspond to "armchair" and "zigzag" nanotubes, respectively. The CrI_3 tubes of (n, n) and (n, 0) indexes are calculated as a function of the diameter in the interval of 12-55 Å, which corresponds to the range from (3, 3) – (5, 0) to (8, 8) – (15, 0). The total number of atoms in the cells ranged from 80 in the smallest (5, 0) zigzag nanotube to 258 in the largest (8, 8) armchair nanotube. Unlike carbon nanotubes, these tubes consist of three atomic layers. The Cr-I bond lengths are identical in monolayer CrI_3. Obviously, folding the sheet into a tube would lead to decrease of the internal Cr-I bond lengths and angles, whereas increasing external ones. Indeed, the nominal Cr-I bond length in single-layer CrI_3 is 2.732 Å while it changes to ~2.715 and 2.838 Å for inner and outer bonds in the smallest (3, 3) nanotube. Therefore, the difference between inner and outer bonds is ~4.3%. As the diameter of CrI_3 nanotube becomes larger, the difference of inner and outer Cr-I bond length of nanotube becomes less significant (~1.1% in (8, 8) nanotube). One should note that the inner bond lengths remain nearly the same independently on the diameter and chirality of the tubes. Rolling single-layer CrI_3 into a tube induces the distortion of the octahedral field. In fact, all Cr-I bond lengths become different from each other that should eventually affect to magnetic anisotropy properties of the material.

The relative strain energies of nanotubes per formula unit (Fig. 2a) demonstrate the inverse exponential dependence similar to carbon and MoS_2 nanotubes [10,41]. The curves show that the strain energy decreases with increasing the tube diameter. However, the highest in strain energy (3, 3) tube is lower than the same MoS_2 tube [42], and even lower in strain energy than (6, 6) MoS_2 (~0.68 eV), likely due to the slightly larger diameter of the (3, 3) CrI_3 tube (14.45 versus ~8 Å for the (3, 3) MoS_2 tube). With increase in the diameter of a CrI_3 tube, the deformation energy becomes less significant and comparable to deformation energy of CNT [41]. The strain energies of CrI_3 nanotubes of both chiralities demonstrate a high correlation of the strain energy with the nanotube diameter. The results of PBE and PBE+U calculations are identical to each other. Thus, the inclusion of the correlation parameter practically does not affect the energy characteristics of the CrI_3 tubes. It is possible to extrapolate the dependence of the strain energy on the tube diameter by fitting the curves. As can be seen in Figure 2a, the tubes with a diameter larger than 45 Å have the strain energies below 0.05 eV/formula unit indicating their synthesis energetically possible. It is worth to note that the smallest diameter of the experimentally produced MoS_2 nanotubes is less than 1 nm [43], and the corresponding deformation energy is ~0.5-0.6 eV/formula unit [10].

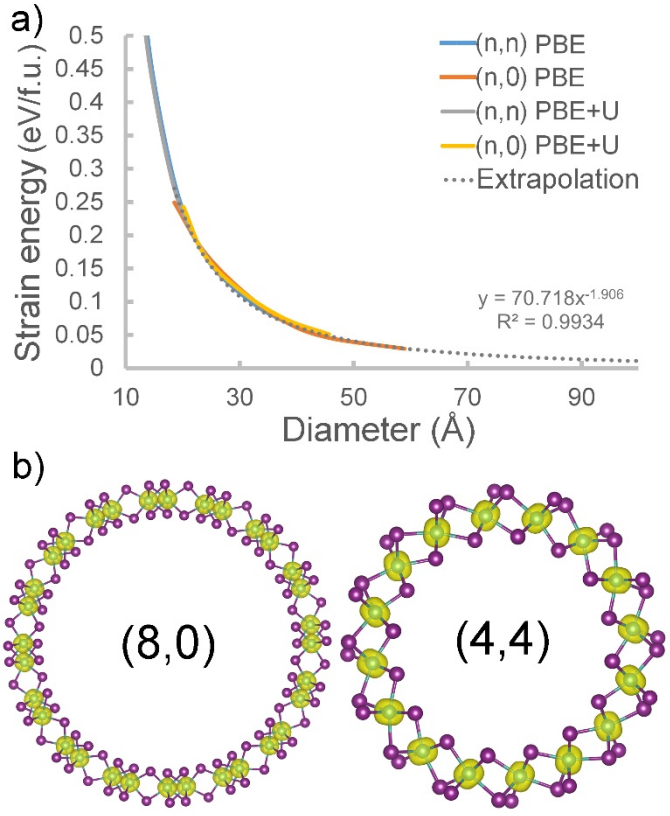

FIG. 2. (a) Relative strain energies (eV/formula unit) upon the diameter (Å) of CrI_3 nanotubes of different chiralities in respect to the CrI_3 monolayer. (b) Spatial distribution of spin density in (8,0) and (4,4) CrI_3 nanotubes.

The spin densities in the nanotubes are mainly distributed over Cr ions with the magnetic moments of 3.09-3.13 μ_B depending on the dimeter of NTs that is in excellent correlation with those of monolayer CrI_3 measured experimentally [27,28], whereas I ions demonstrate a residual opposite sign of magnetization of $\sim -0.07\ \mu_B$ (Fig. 2b). Including the PBE+U correction enhances Cr magnetic moments up to ~3.37-3.41 μ_B, while I atoms demonstrate almost twice increase of the moments up to ~ -0.12-$0.14\ \mu_B$. Generally magnetic moments do not depend strictly on the tube dimeter and slightly increased with smaller diameters due to the alteration of Cr-I bond lengths.

To demonstrate how electronic structure of the tubes affected by wrapping with respect to the CrI_3 sheet, we first calculate the electronic structure of the monolayer (Fig. 3a). The band structures show that the CrI_3 monolayer is a ferromagnetic semiconductor with direct spin-up and indirect spin-down band gaps that is in good agreement with known experimental and theoretical data [14,44]. Taking into account of U parameter in terms of DFT+U formalism significantly enhances the spin-down band gap and is in better (compared to pure PBE) agreement to the band structure calculated within the hybrid Heyd-Scuseria-Ernzerhof (HSE06) functional [45,46] (Fig. 3a, right). The lowest spin-up conduction band (CB) states calculated within PBE+U lie around 1 eV (Figure 3a, middle panel) whereas the spin-down CB states are located at higher energies around 2.8 eV.

The electronic structures of the nanotubes also reveal their ferromagnetic semiconducting behavior. The widths of the band gaps in the tubes (Fig. 3b) are slightly smaller than that in the monolayer due to wrapping-induced distortions in bond lengths. It is important to note, that (*n, n*) nanotubes demonstrate indirect-direct band gap transition in spin-down states, while (*n, 0*) tubes show inverse direct to indirect band gap transition in the spin-up channel. Thus, (*n, n*) nanotubes are direct semiconductors in both spin channels. Similarly to the monolayer, the PBE+U approximation affects the electronic structure of CrI_3 nanotubes, increasing the spin-down band-gaps (Fig. 3c). Since even the smallest cell of calculated nanotubes contains 80 atoms, it is quite difficult to adopt the HSE06 functional for calculation of their electronic structure. However, because of CrI_3 nanotubes represent the folded monolayer, the band gap correction should follow that of the monolayer. Reducing the diameter of tubes leads to decrease in band gaps (Fig. 3c) due to a stronger distortion of the Cr-I crystal field. A similar change in properties was previously found for MoS_2 nanotubes [10]. Thus, the semiconducting magnetic CrI_3 nanotubes can be used to generate contact-induced spin polarization in low-dimensional materials [47] or in the purpose of effective valley splitting [26].

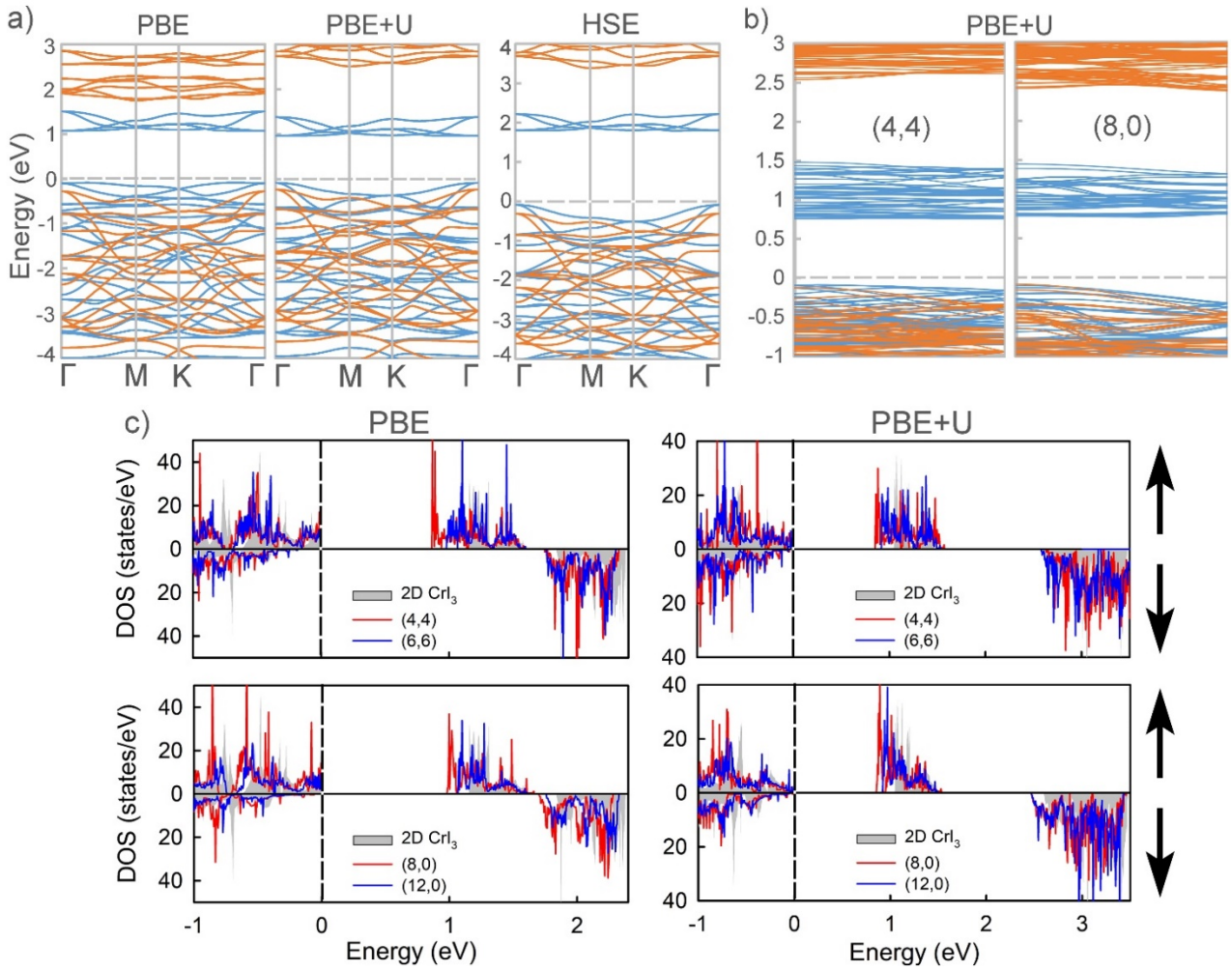

FIG. 3. (a) Band structure of the CrI_3 monolayer calculated using PBE (left), PBE+U (middle) and HSE06 (right) functionals. The blue and red lines correspond to spin-up and spin-down states respectively. (b) Band structure of (4, 4) and (8, 0) CrI_3 nanotubes calculated at PBE+U level of theory. (c) Total densities of states of CrI_3 nanotubes at PBE (left) and PBE+U (right) levels of theory. Blue and red lines denote nanotubes of different diameters while gray shaded area represents DOS of single-layer CrI_3. The black arrows represent spin-up and spin-down states for respective DOS. The Fermi level is set to 0 eV.

The variations of magnetic moments under loaded stress and strain are to be negligible (up to 0.03 μ_B) and is in good correlation with results on the study of monolayer CrI_3 under moderate strain [48]. Two papers recently reported strain-tunable electronic properties of single-layer CrI_3 [49,50], which are controversial to each other at least in FM-AFM transition. Webster and Yan demonstrated the phase transition from FM to AFM when compression more than 5.7% is applied [49], while Wu et al. found that such transition occurs at around 1.8% of uniaxial strain [50]. We calculated the total energies of the nanotubes for both FM and AFM configurations (Fig. 4a) and found absence of the FM to AFM magnetic phase transition in the studied range of applied strain suggesting a possible path to stabilization the magnetic phase in strained CrI_3. Moreover, the

exchange energy growths with stretching, that should reflects in enhancing magnetic anisotropy and, in particular, Curie temperature. Applied strain leads to deformation in the band gaps. The variation of band gap with respect to the applied tensile strain (Fig. 4b) reveals nontrivial dependence in (4, 4) nanotubes. Upon expansion, nanotubes of both chiralities reveal nearly linear large increase of the spin-down band gaps, while the spin-up gaps is decreased moderately. Meanwhile, under compression, the (4, 4) tube exhibits decrease of both spin-up and spin-down band gaps demonstrating its nontrivial behavior whereas the band gaps of (8, 0) reveal tendency opposite to expansion. The nontrivial behavior is attributed to the evolution of structural parameters in the Cr-I octahedral field, which becomes more distorted in (4, 4) compared to (8, 0) nanotubes under compression affecting spin states of the material.

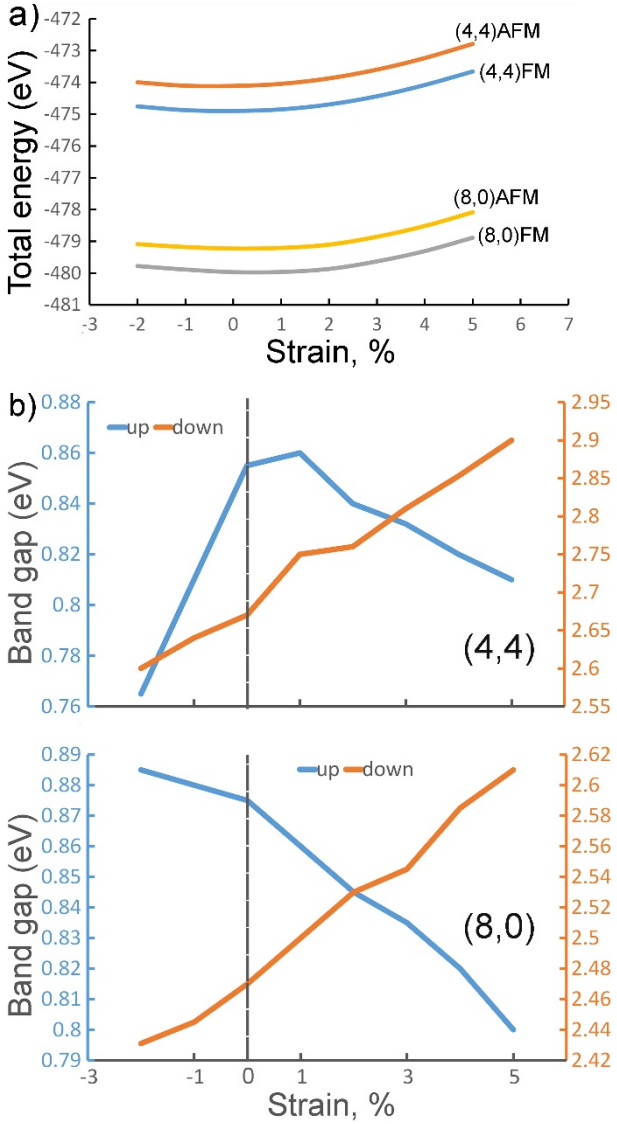

FIG. 4. (a) Strain effect on the total energy of CrI_3 magnetic nanotubes. (b) Spin-up (in blue) and spin-down (in red) band gaps with respect to the applied strain in (4, 4) and (8, 0) CrI_3 nanotubes.

For low-dimensional systems, such as CrI_3 nanotubes and monolayer, the stability of magnetic long-range order is directly linked to magnetic anisotropy because of the Mermin-Wagner theorem. However, the origins of magnetic anisotropy in CrI_3 monolayers are rather complicated and not so clear yet. In Ref. [51], it was proposed that the anisotropy of the exchange parameter causes predominant "out of plane" orientation of magnetic moments. Our calculations also show that the exchange energies for "out-of-plane" and "in-plane" CrI_3 monolayer magnetic configurations vary by up to 10 %, which may result in magnetic anisotropy energy (MAE) in the order of ~1 meV/atom. On the other hand, it was proven [52] that next nearest-neighbor Dzyaloshinskii-Moriya interaction is present in CrI_3. Furthermore, breaking of translational symmetry and rolling of single-layer CrI_3 into a nanotube can result in much more complicated magnetic behavior, which should be discussed in further study. Indeed, thermomagnetic properties of magnetic materials strongly depend on the exchange interactions of electron and magnetic spin moments. Recent Metropolis MC simulation of zigzag and armchair type CrI_3 nanotube demonstrated different thermomagnetic responses depending on the chirality and diameter of the nanotubes [53]. It has been shown that the Curie temperature of zigzag CrI_3 nanotubes increases twice with doubling diameter and could much exceed that of the monolayer. However, increase of nanotube diameter should make thermomagnetic properties to be closer to that of the monolayer that is controversial to the recent results. Finally, the Curie temperature of nanotubes of large diameter should not exceed that of monolayer CrI_3. Therefore, we believe that thermomagnetic properties of CrI_3 nanotubes are still an open question and this topic is of a distinct complex study.

IV. CONCLUSIONS

In conclusion, structural, energetic and electronic properties of CrI_3 nanotubes with different chirality and diameter were studied. A high correlation of the strain energy with the nanotube diameter was demonstrated at both PBE and PBE+U levels of theory. Tubes of large diameter have strain energies below 0.05 eV/formula unit proposing their synthesis energetically possible. The results suggest that nanotubes of both chiralities are ferromagnetic semiconductors with the band gaps close to that of the monolayer. Internal structural stresses of CrI_3 NTs and changes in bond lengths lead to a distortion of the Cr-I octahedral field resulting in suppression of band gaps as the tube diameter reduces. The electronic properties of CrI_3 NTs can be tuned by an external strain with a flexible spin-up/spin-down band gap ratio. Under compression, the (4, 4) tube exhibits decrease of the spin-up and spin-down band gap demonstrating its nontrivial behavior resulted from the strong

distortion of the Cr-I octahedral field. Thus, the desirable properties of CrI_3 NTs can be controlled for potential application in spintronic devices.

ACKNOWLEDGMENTS

This work is supported by the government contract of the Ministry of Education and Science of the Russian Federation to Siberian Federal University (Grant No. 16.1455.2017/PCh). The authors thanks the Irkutsk Supercomputer Center of SB RAS for providing access to HPC-cluster "Akademik V.M. Matrosov". A.V.K. acknowledges the US Air Force Office of Scientific Research (contract FA-9550-18-1-0032), W.B. and P.V.A. acknowledge National Research Foundation of Republic of Korea for support under grant NRF-2017R1A2B400440.

References

[1] S. Iijima, Nature **354**, 56 (1991).

[2] T. W. Ebbesen and P. M. Ajayan, Nature **358**, 220 (1992).

[3] M. S. Dresselhaus, G. Dresselhaus, and P. C. Eklund, *Science of Fullerenes and Carbon Nanotubes* (1996).

[4] D. Golberg, Y. Bando, M. Eremets, K. Takemura, K. Kurashima, and H. Yusa, Appl. Phys. Lett. **69**, 2045 (1998).

[5] N. G. Chopra, R. J. Luyken, K. Cherrey, V. H. Crespi, M. L. Cohen, S. G. Louie, and A. Zettl, Science. **269**, 966 (1995).

[6] A. Loiseau, F. Willaime, N. Demoncy, G. Hug, and H. Pascard, Phys. Rev. Lett. **76**, 4737 (1996).

[7] R. R. Chianelli, E. B. Prestridge, T. A. Pecoraro, and J. P. Deneufville, Science. **203**, 1105 (1979).

[8] R. Tenne, L. Margulis, M. Genut, and G. Hodes, Nature **360**, 444 (1992).

[9] L. Margulis, G. Salitra, R. Tenne, and M. Talianker, Nature **365**, 113 (1993).

[10] G. Seifert, H. Terrones, M. Terrones, G. Jungnickel, and T. Frauenheim, Phys. Rev. Lett. **85**, 146 (2000).

[11] G. Seifert, H. Terrones, M. Terrones, G. Jungnickel, and T. Frauenheim, Solid State Commun. **114**, 245 (2000).

[12] N. Zibouche, A. Kuc, and T. Heine, Eur. Phys. J. B **85**, 49 (2012).

[13] C. Gong, L. Li, Z. Li, H. Ji, A. Stern, Y. Xia, T. Cao, W. Bao, C. Wang, Y. Wang, Z. Q. Qiu, R. J. Cava, S. G. Louie, J. Xia, and X. Zhang, Nature **546**, 265 (2017).

[14] B. Huang, G. Clark, E. Navarro-Moratalla, D. R. Klein, R. Cheng, K. L. Seyler, D. Zhong, E.

Schmidgall, M. A. McGuire, D. H. Cobden, W. Yao, D. Xiao, P. Jarillo-Herrero, and X. Xu, Nature **546**, 270 (2017).

[15] H. Wang, V. Eyert, and U. Schwingenschlögl, J. Phys. Condens. Matter **23**, 116003 (2011).

[16] Y. Sun, Z. Zhuo, X. Wu, and J. Yang, Nano Lett. **17**, 2771 (2017).

[17] A. V. Kuklin, A. A. Kuzubov, E. A. Kovaleva, N. S. Mikhaleva, F. N. Tomilin, H. Lee, and P. V. Avramov, Nanoscale **9**, 621 (2017).

[18] X. Li, X. Wu, and J. Yang, J. Am. Chem. Soc. **136**, 11065 (2014).

[19] A. V. Kuklin, S. A. Shostak, and A. A. Kuzubov, J. Phys. Chem. Lett. **9**, 1422 (2018).

[20] M. Bonilla, S. Kolekar, Y. Ma, H. C. Diaz, V. Kalappattil, R. Das, T. Eggers, H. R. Gutierrez, M.-H. Phan, and M. Batzill, Nat. Nanotechnol. **13**, 289 (2018).

[21] N. Sethulakshmi, A. Mishra, P. M. Ajayan, Y. Kawazoe, A. K. Roy, A. K. Singh, and C. S. Tiwary, Mater. Today (2019).

[22] D. J. O'Hara, T. Zhu, A. H. Trout, A. S. Ahmed, Y. K. Luo, C. H. Lee, M. R. Brenner, S. Rajan, J. A. Gupta, D. W. McComb, and R. K. Kawakami, Nano Lett. **18**, 3125 (2018).

[23] Y. Zhao, J. Zhang, S. Yuan, and Z. Chen, Adv. Funct. Mater. 1901420 (2019).

[24] T. Song, X. Cai, M. W.-Y. Tu, X. Zhang, B. Huang, N. P. Wilson, K. L. Seyler, L. Zhu, T. Taniguchi, K. Watanabe, M. A. McGuire, D. H. Cobden, D. Xiao, W. Yao, and X. Xu, Science. **360**, 1214 (2018).

[25] D. Zhong, K. L. Seyler, X. Linpeng, R. Cheng, N. Sivadas, B. Huang, E. Schmidgall, T. Taniguchi, K. Watanabe, M. A. McGuire, W. Yao, D. Xiao, K.-M. C. Fu, and X. Xu, Sci. Adv. **3**, e1603113 (2017).

[26] Z. Zhang, X. Ni, H. Huang, L. Hu, and F. Liu, Phys. Rev. B **99**, 115441 (2019).

[27] S. Jiang, L. Li, Z. Wang, K. F. Mak, and J. Shan, Nat. Nanotechnol. **13**, 549 (2018).

[28] M. A. McGuire, H. Dixit, V. R. Cooper, and B. C. Sales, Chem. Mater. **27**, 612 (2015).

[29] W.-B. Zhang, Q. Qu, P. Zhu, and C.-H. Lam, J. Mater. Chem. C **3**, 12457 (2015).

[30] W. Kohn and L. J. Sham, Phys. Rev. **140**, A1133 (1965).

[31] P. Hohenberg, Phys. Rev. **136**, B864 (1964).

[32] J. P. Perdew, J. A. Chevary, S. H. Vosko, K. A. Jackson, M. R. Pederson, D. J. Singh, and C. Fiolhais, Phys. Rev. B **46**, 6671 (1992).

[33] J. P. Perdew, K. Burke, and M. Ernzerhof, Phys. Rev. Lett. **77**, 3865 (1996).

[34] V. I. Anisimov, J. Zaanen, and O. K. Andersen, Phys. Rev. B **44**, 943 (1991).

[35] S. L. Dudarev, S. Y. Savrasov, C. J. Humphreys, and A. P. Sutton, Phys. Rev. B **57**, 1505 (1998).

[36] G. Kresse and J. Furthmüller, Comput. Mater. Sci. **6**, 15 (1996).

[37] G. Kresse and J. Hafner, Phys. Rev. B **47**, 558 (1993).

[38] S. W. Jang, M. Y. Jeong, H. Yoon, S. Ryee, and M. J. Han, Phys. Rev. Mater. **3**, (2019).

[39] S. Grimme, J. Antony, S. Ehrlich, and H. Krieg, J. Chem. Phys. **132**, 154104 (2010).

[40] H. J. Monkhorst and J. D. Pack, Phys. Rev. B **13**, 5188 (1976).

[41] E. Hernández, C. Goze, P. Bernier, and A. Rubio, Phys. Rev. Lett. **80**, 4502 (1998).

[42] G. Seifert, H. Terrones, M. Terrones, G. Jungnickel, and T. Frauenheim, Phys. Rev. Lett. **85**, 146 (2000).

[43] M. Remskar, A. Mrzel, Z. Skraba, A. Jesih, M. Ceh, J. Demsar, P. Stadelmann, F. Levy, and D. Mihailovic, Science. **292**, 479 (2001).

[44] W.-B. Zhang, Q. Qu, P. Zhu, and C.-H. Lam, J. Mater. Chem. C **3**, 12457 (2015).

[45] J. Heyd, G. E. Scuseria, and M. Ernzerhof, J. Chem. Phys. **118**, 8207 (2003).

[46] A. V. Krukau, O. A. Vydrov, A. F. Izmaylov, and G. E. Scuseria, J. Chem. Phys. **125**, 224106 (2006).

[47] A. V. Kuklin, A. A. Kuzubov, E. A. Kovaleva, H. Lee, P. B. Sorokin, S. Sakai, S. Entani, H. Naramoto, and P. Avramov, J. Magn. Magn. Mater. **440**, 23 (2017).

[48] T. Mukherjee, S. Chowdhury, D. Jana, and L. C. L. Y. Voon, J. Phys. Condens. Matter **31**, 335802 (2019).

[49] L. Webster and J.-A. Yan, Phys. Rev. B **98**, 144411 (2018).

[50] Z. Wu, J. Yu, and S. Yuan, Phys. Chem. Chem. Phys. **21**, 7750 (2019).

[51] J. L. Lado and J. Fernández-Rossier, 2D Mater. **4**, 035002 (2017).

[52] L. Chen, J.-H. Chung, B. Gao, T. Chen, M. B. Stone, A. I. Kolesnikov, Q. Huang, and P. Dai, Phys. Rev. X **8**, 041028 (2018).

[53] M. Moaied and J. Hong, Nanomaterials **9**, 153 (2019).